

# A STUDY OF CLIMATOLOGICAL ASPECTS OF FLOW FIELD AND HEAT EXCHANGE ON TROPICAL PACIFIC SURFACE IN THE EL NINO AND LA NINA EVENTS

Ma Kaiyu (马开玉), Pan Yinong (泮益农)

Department of Atmospheric Sciences, Nanjing University, Nanjing 210093

and Jiang Dayong (姜达雍)

Chinese Academy of Meteorological Sciences, Beijing 100081

Received August 5, 1994; revised January 29, 1995

## ABSTRACT

In this paper, based on the  $2^{\circ} \times 2^{\circ}$  grid data COADS from 1950—1987 the flow field and heat exchange anomalies on the tropical ( $11^{\circ}\text{S}$ — $11^{\circ}\text{N}$ ,  $120^{\circ}\text{E}$ — $80^{\circ}\text{W}$ ) Pacific surface (TPS) are studied in El Nino and La Nina events. During El Nino, the zonal pressure gradient and the trade winds decrease on the TPS, the tropical convergence strengthens on the TPS, especially on the central TPS, the sensible and latent heat exchanges increase, the net longwave radiation and incident solar radiation decrease and the net gain (loss) of heat reduces (increases) on the central and eastern TPS. During La Nina the results turn out the contrary. Finally, two feedback mechanisms which include the dynamic, thermal and hydrological processes during El Nino and La Nina are summarized and a conceptive model for El Nino-La Nina cycle is given.

**Key words:** flow field, heat exchange anomalies, El Nino, La Nina

## I. INTRODUCTION

Large scale air-sea interaction plays a crucial role in climate change and variability on a broad range of time scales. The most prominent signal in the tropics on interannual time scale is the El Nino event during which anomalous warm surface water appears for a number of months in the central and eastern tropical Pacific (TP). Numerous studies have suggested that the El Nino events could bring about severe climate abnormality and create severe flood, drought, low temperature and frozen disasters in certain regions. Therefore the meteorologists and oceanographers in the world focus their attention on the studies on El Nino events in an attempt to provide reliable information and physical evidence for the prediction of El Nino occurrence and climate disasters in the future.

Bjerknes (1966) first suggested that the equatorial easterlies weakened and disappeared temporarily over the central and eastern Pacific during the El Nino process. Data analysis and numerical modeling indicate that the drought belt weakened and shrunk and precipitation increased in the central and eastern TP when sea surface temperature (SST) rose abnormally in the cold tongue region (Rowntree 1977; Wang et al. 1986). Ramage and Hori (1981) computed the  $v$ -component of the wind and heat budget in April 1972—March 1973 El Nino period and January—March 1972 and April—December 1973 non El

Nino periods on the surface from the eastern TP to the Date Line (15°S—15°N). They found that the speed of  $v$ -component in non-El Nino period was higher than that in the El Nino period to the north of the equatorial Pacific and that the maximum difference in heat budget between El Nino and non-El Nino appeared in the southern tropical ocean. Zhu and Yang (1990) found that the distributions of sensible and latent heat fluxes in the Indian Ocean were similar to that in normal years after they analysed the heat fluxes in the tropical Pacific and Indian Oceans in the developing and ending months of 1982—1983 El Nino event. Ma et al. (1993) suggested that the differences of the components of heat budget between El Nino and La Nina mainly appeared on the TPS especially on the central and eastern TPS from the analyses of heat budgets on TPS in 1987 El Nino and 1974 La Nina periods.

These researches have provided useful references for the understanding of the air-sea system interaction during abnormal SST in the TP, but they came from the analyses of the individual typical abnormal SST events. Based on more data, the present work is to provide the flow field and heat exchange anomalies in El Nino and La Nina events in an attempt to improve the understanding of the air-sea coupling mechanism in El Nino-La Nina cycle and the related climate modeling. The data used are described in Section II along with the method. The flow field and the heat exchange anomalies are presented in Sections III and IV respectively. Two feedback mechanisms in El Nino-La Nina cycle are given in Section V. Finally, some conclusions are presented in Section VI.

## II. DATA AND METHOD

Based on the  $2^\circ \times 2^\circ$  grid data COADS, the pressure, wind, temperature, humidity and cloud from 1950 to 1987 are used to compute the averages and the differences of the pressure, zonal wind, meridional wind, and the components of heat budget between El Nino and La Nina on the Pacific surface (11°S—11°N, 120°E—80°W), the flow field and heat budget are analysed. The El Nino and La Nina events in Table 1 are taken from the Monitoring Group of ENSO (1989).

**Table 1.** El Nino and La Nina Events (based on the Monitoring Group of ENSO, 1989) \*

El Nino		La Nina	
1951. 8—1952. 4	1953. 4—1953. 10	1954. 6—1956. 7	1964. 4—1964. 12
1957. 4—1958. 8	1963. 7—1964. 1	1967. 7—1968. 6	1970. 8—1971. 12
1965. 5—1966. 3	1968. 10—1970. 1	1973. 9—1975. 1	1975. 5—1976. 3
1972. 6—1973. 3	1976. 6—1977. 3	1984. 10—1985. 9	
1982. 9—1983. 9	1986. 10—1988. 3		

\* The Monitoring Group of ENSO (1989) defined the El Nino (La Nina) event as a warm (cold) ocean event with the mean monthly SST deviation of  $\Delta T \geq 0.5^\circ\text{C}$  ( $\leq -0.5^\circ\text{C}$ ) and the duration of month  $\geq 6$  in the area of 10°S to 0° and 180° to 90°W. The discontinuous period is  $\leq 1$  month.

The sensible and latent heat exchanges are given by

$$Q_c = \rho C_d C_p (T_s - T_a) V, \quad (1)$$

$$Q_c = \rho C_d L (q_s - q_a) V, \quad (2)$$

where  $\rho=1.175 \text{ kg m}^{-3}$  is air density,  $C_p$  the specific heat at constant pressure,  $L$  the latent heat evaporation,  $T_s$  and  $T_a$  the SST and air temperature,  $q_a$  and  $q_s$  the surface specific humidity and the saturation specific humidity corresponding to the SST,  $V$  the scalar mean wind speed,  $C_d$  the exchange coefficient related to wind speed and stability (Bunker 1976).

Following Budyko (1958) and Ramage and Hori (1981), net longwave radiation and incident solar radiation fluxes are computed by

$$Q_1 = \epsilon \delta T_a^4 (0.39 - 0.056 \sqrt{q_a}) (1 - bn^2) + 4\epsilon \delta T_a^3 (T_s - T_a), \quad (3)$$

$$Q_s = Q_o (1 - (a + bn)n) (1 - r), \quad (4)$$

where  $\sigma$  is Stefan-Boltzmann constant,  $\epsilon=1$  the emissivity,  $n$  the fraction of total cloud cover,  $a$  and  $b$  are the parameter varying with latitude,  $Q_o$  the average monthly total solar radiation flux at the sea surface under clear sky and  $r$  the average albedo of sea surface to solar radiation. Their values are based on Budyko (1974). The heat budget is obtained by

$$Q_b = Q_s (Q_c + Q_e + Q_1). \quad (5)$$

Ocean and atmosphere are coupled through dynamic, thermal and hydrological processes with varieties of interrelated and interacted space and time scales. Therefore the following results are the outgrowth of the air-sea coupling and interactions of different space and time scales.

### III. FLOW FIELD

#### (1) Pressure

The distributions of sea surface pressure were characterized by a high center in the south of the eastern TP and a low center in the warm pool of the western TP. The difference between the eastern high and the western low was about 5 hPa. Figure 1 shows the distributions of the pressures in El Nino and La Nina events and their differences. It could be seen that during El Nino (La Nina) the pressure decreased (increased) in the eastern TP and increased (decreased) in the western TP. The positive center of the differences with 1.5 hPa appeared on the southern side of the western TP and a large negative region below 1.0 hPa was located near the western coast of the equator. They suggested that the zonal pressure gradient decreased during El Nino and increased during La Nina.

#### (2) Zonal and Meridional Winds

Trade wind anomalies in the TP play a crucial role in the El Nino and La Nina developments. Figures 2 and 3 show the zonal and meridional winds in El Nino and La Nina and their differences respectively.

In Fig. 2a, it could be seen that the significant feature is the domination of east wind throughout the TP, which drives the cold Peru current to move westward along the equator. A large value belt over  $4 \text{ m s}^{-1}$  appears from the middle TP to the western coast of Peru. It suggests that there are zonal wind convergence and divergence on the western and eastern sides of the belt respectively. During El Nino, the east (west) wind remarkably weakens (strengthens) in the TP from  $150^\circ\text{E}$  to  $120^\circ\text{W}$ , as compared with La Nina. From Fig. 2b it could be seen that the largest difference of zonal winds between El Nino and La Nina is in the central TP. They suggest that during El Nino the zonal wind convergence has an eastward movement in the middle TP and the upwelling and westward movement of

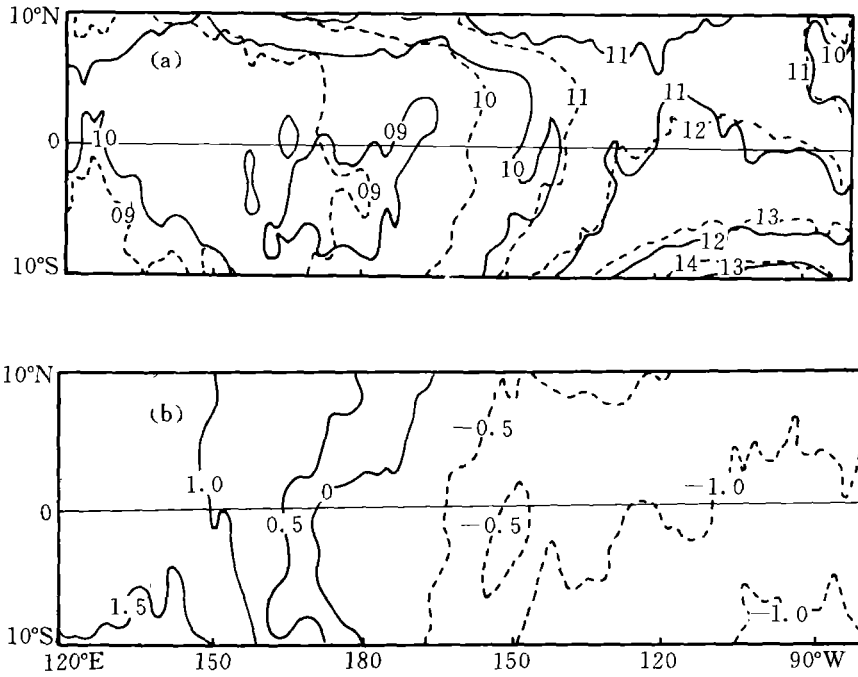


Fig. 1. Sea surface pressures (a) averaged in El Niño (solid line) and La Niña (broken line) and their difference (b) (units: hPa, and in (a) 10 represents 1010 and 09 represents 1009).

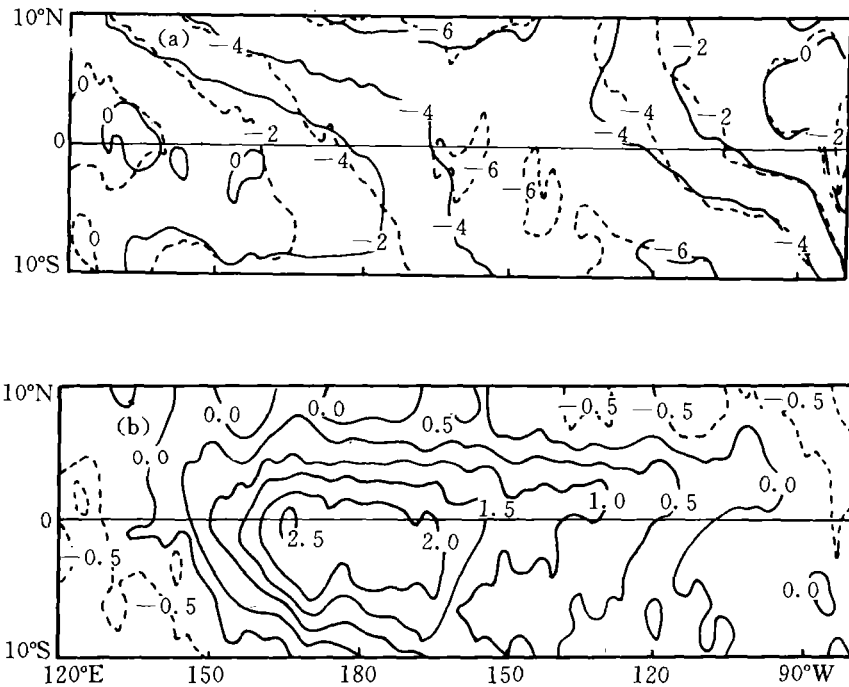


Fig. 2. Zonal winds (a) averaged in El Niño (solid line) and La Niña (broken line) and their difference (b) (units:  $\text{m s}^{-1}$ ).

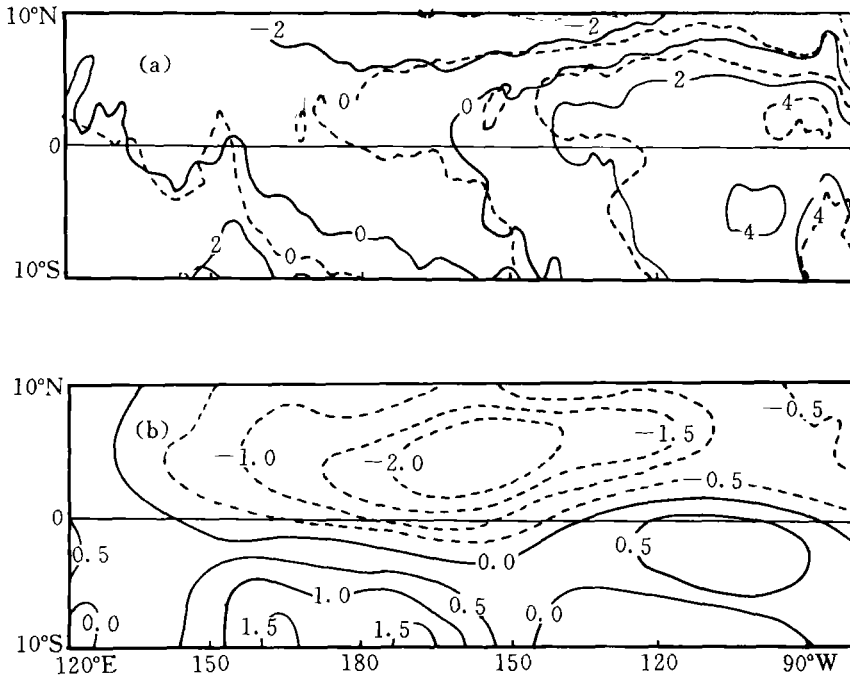


Fig. 3. As in Fig. 2 except for meridional wind.

cold water in the eastern TP are restrained due to the strengthening of the west wind in TP.

In Fig. 3a, it could be seen that in the eastern TP there prevailed the south wind with the maximum of  $4 \text{ m s}^{-1}$  near the coast of Peru and Ecuador and that during El Nino the north wind increased on the northern side of TP and decreased on the southern side of the TP in comparison with La Nina. Therefore during El Nino the tropical convergence strengthened throughout the TP, especially in the middle TP, as it could be seen in Fig. 3b that the differences between El Nino and La Nina were positive on the southern side of the TP and negative on the northern side of the TP. During El Nino the north wind increased by  $2 \text{ m s}^{-1}$  on the northern side of the central TP and the south wind increased by  $1.5 \text{ m s}^{-1}$  on the southern side of the central TP at maximum as compared with La Nina. During El Nino the strengthening of the north wind on the northern side of the TP especially in the eastern TP, which coincided with the result of Ramage and Hori (1981), facilitated the maintenance of the cold water upwelling there.

#### IV. HEAT EXCHANGE

Heat exchange on the tropical ocean surface is an inseparable part of the general circulation and the global heat budget. The heat gained by the tropical ocean is released largely to heat the tropical atmosphere while a portion of the heat is released into the atmosphere in high latitudes by ocean current transport. The heat fluxes released from the ocean surface largely depend on and affect the SST.

##### (1) Sensible Heat

In contrast with other elements of the heat budget, the sensible heat flux is relatively

small in the tropical ocean. In the vast TP the sensible heat fluxes range from  $-5$  to  $10 \text{ W m}^{-2}$  with high values in the warm pool and low ones in the cold tongue.

During La Nina the negative flux of sensible heat, meaning the slight downward heat transfer, featured the southern side of the eastern TP. During El Nino the negative flux area shrank eastward towards the coast of Peru.

The differences in sensible heat fluxes between El Nino and La Nina were about  $-3$  to  $5 \text{ W m}^{-2}$  throughout the TP and positive from the central TP to the western coast of Peru. But on the west side of the warm pool and the northern side of the eastern TP the differences were negative.

### (2) Net Longwave Radiation

From (3) the factors affecting the net longwave radiation are cloud cover, specific humidity and air-sea temperature difference besides the sea surface air temperature. Therefore the response of the net longwave radiation to SST could be very complicated under the air-sea coupling and interaction.

Although the net longwave radiation fluxes, which ranged from  $60$  to  $80 \text{ W m}^{-2}$  on TPS, were much larger than the sensible heat fluxes, the differences between El Nino and La Nina were about  $-5$  to  $3 \text{ W m}^{-2}$ , almost being of the same order of magnitude as the differences of sensible heat fluxes. On the vast TPS from the central TP to the western coast of Peru the net longwave radiation decreased during El Nino and increased during La Nina and their differences were negative. It could be explained that the evaporation increased (decreased), and the water vapor and cloud amount increased (reduced) so as to cause the reduction (increase) of net longwave radiation when SST rose (declined) abnormally.

### (3) Latent Heat

From (2), if the air density is constant, the control factors of latent heat exchange will be the drag coefficient, wind speed and vertical gradient of specific humidity on the sea surface. The fluctuation of SST could influence these elements under the air-sea interaction.

Figure 4 displays the latent heat fluxes averaged in El Nino and La Nina events and their difference. In contrast with the sensible and longwave radiation fluxes, the latent heat flux is the largest component of heat loss from the ocean to the atmosphere in the tropical ocean. As compared with La Nina, during El Nino more latent heat was released on the ocean surface from the eastern part of the central TP to the western coasts of Ecuador and Peru, but less in the area around the Date Line mainly due to the reduction of zonal wind there (see Fig. 2). The difference of the fluxes between El Nino and La Nina had a broad range from  $-25$  to  $35 \text{ W m}^{-2}$  about 8 times larger than the differences of sensible heat and net longwave radiation fluxes.

### (4) Incident Solar Radiation

Although the incident solar radiation on the ocean surface depends on total solar radiation under clear sky  $Q_0$ , coefficient  $a$ , albedo  $r$  and cloud amount  $n$ , the difference of the fluxes between El Nino and La Nina mainly depends on cloud due to  $Q_0$ ,  $a$  and  $r$  varying with latitude.

Figure 6 represents the incident solar radiation fluxes averaged in El Nino and La Nina

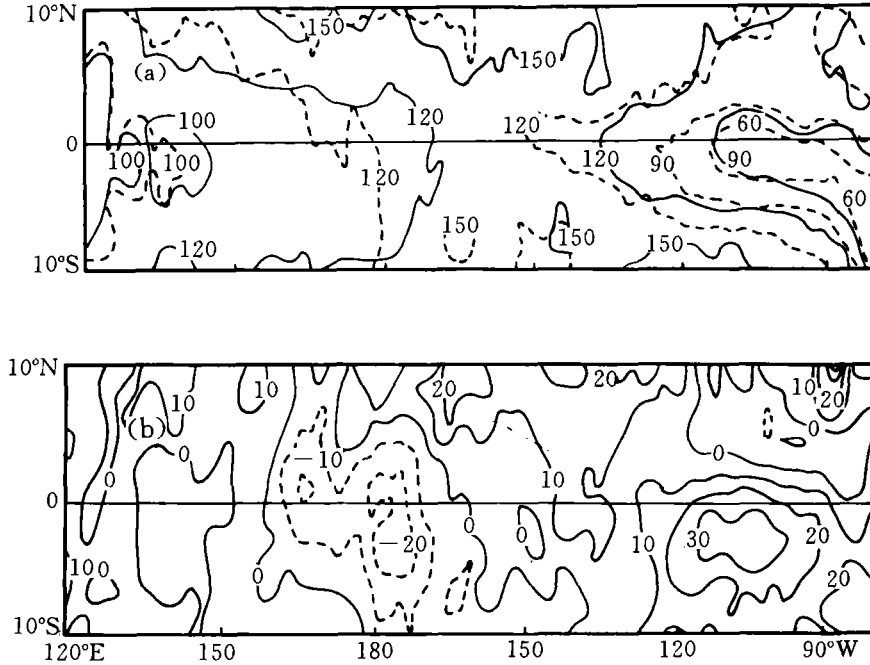


Fig. 4. As in Fig. 2 except for latent heat, in  $W m^{-2}$ .

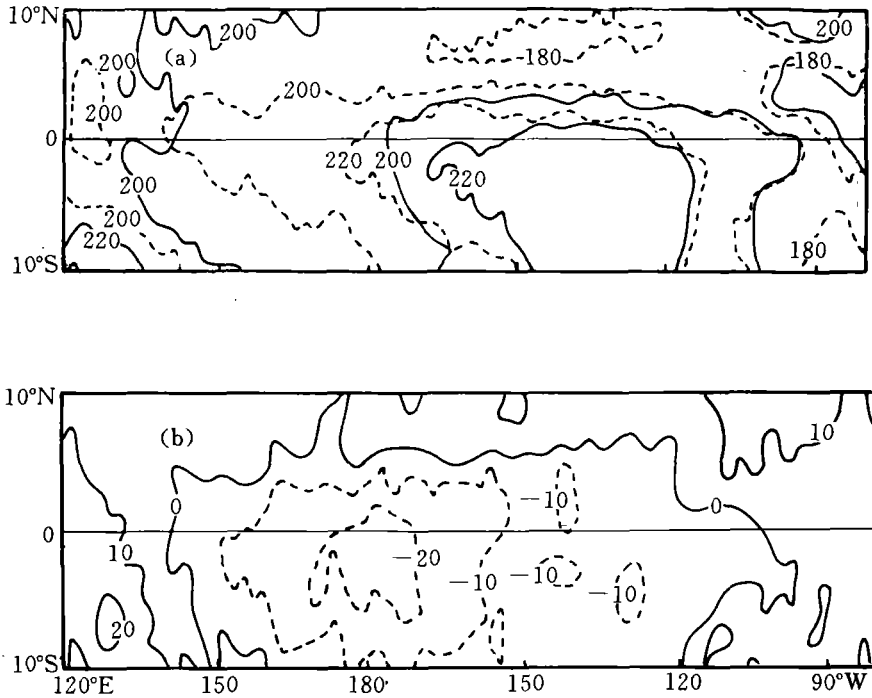


Fig. 5. As in Fig. 4 except for incident solar radiation.

and their difference. It reveals that in the vast tropical ocean the incident solar radiation fluxes in El Nino were less than those in La Nina and the difference of the fluxes between El Nino and La Nina was characterized by a broad negative value area on the TPS.

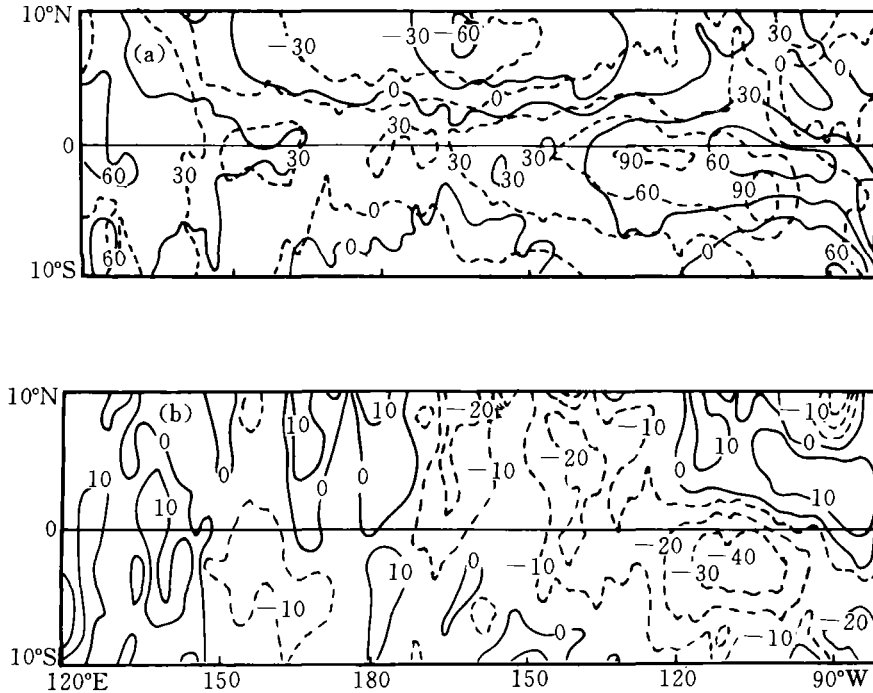


Fig. 6. As in Fig. 4 except for heat budget.

especially on the central TPS around the Date Line where the negative difference reached  $-20 W m^{-2}$ , this is because that when SST rose abnormally the airflow convergence and evaporation increased on the ocean surface, and the water vapor content and instability grew in the atmosphere so as to cause an increase of cloud which results in the reduction of incident solar radiation.

##### (5) Heat Budget

On the ocean surface heat budget depends on the solar radiation absorbed and the total energy released. The anomalies of latent heat and incident solar radiation fluxes are the major factors controlling the heat budget variations. The differences of sensible heat and longwave radiation fluxes between El Niño and La Niña were relatively small and their signs were often opposite during El Niño and La Niña. Hence the distributions of heat budgets between El Niño and La Niña and their difference on the TPS largely reflect the latent heat and incident solar radiation fluxes.

In Fig. 6a, it is featured that on the central TPS the heat budgets averaged in El Niño and La Niña ranged from  $-60$  to  $30 W m^{-2}$  much less than those on the western and eastern TPS where the budgets were  $30$  to  $60 W m^{-2}$  generally. In Fig. 6b there appeared negative values on the ocean surface from the central TP to the western coast of Peru where the negative difference reached  $-30$  to  $-40 W m^{-2}$ , meaning that the net gain (loss) of heat flux was less (more) in El Niño as compared with that in La Niña.

## V. TWO FEEDBACK MECHANISMS

From the above analyses, during El Niño processes the pressure gradient and trade wind decreased on TPS, the tropical convergence strengthened on TPS especially on the

central TPS, the sensible and latent heat exchanges increased on the central-eastern TPS, the net longwave radiation and incident solar radiation reduced, and so the net gain (loss) of heat flux decreased (increased) on the ocean surface from the central TPS to the western coast of Peru. During La Nino, the opposites were found. Therefore in El Nino-La Nino cycle the following two air-sea coupling feedback mechanisms may be summarized:

On the TPS, the weakening of pressure gradient and trade winds would bring about the eastward expanding of the warm pool water and restrain the cold tongue water upwelling and westward movement, as a result the surface water temperature in the eastern TP will rise. The rising of the surface water temperature in the eastern TP would further cause the weakening of the pressure gradient and the trade winds, the eastward expanding of the warm pool water, the weakening of the cold water upwelling and westward movement. Consequently the surface water temperature would rise abnormally and El Nino occurs. Otherwise, the circumstances would be opposite and La Nina would occur. This is a positive feedback mechanism Bjerknes (1966) first hypothesized on a descriptive basis. On the other hand, during El Nino the above-normal SST would bring about the increases of tropical convergence, sensible and latent heat exchanges and the rise of water vapor content and instability in the atmosphere, and in turn the growth of cloud cover, which would cause the weakening of net longwave radiation and incident solar radiation. Consequently the net gain (loss) of heat flux would decrease (increase) so decrease to SST, favor the occurrence of La Nina. During La Nina the opposite circumstances would occur to create a favorable condition for El Nino. This is a the negative feedback mechanism. Both the positive and the negative feedback mechanisms interact on and restrain each other. Figure 7 shows the conceptional model of these two feedback mechanisms in El Nino-La Nina cycle.

VI. CONCLUSIONS

Now the following conclusions can be summarized:

(1) During El Nino, the pressure gradient and trade wind decreased on the TPS, the tropical convergence strengthened on TPS especially on the central TPS, the sensible and latent heat exchanges enhanced on the central-eastern TPS, the net longwave radiation

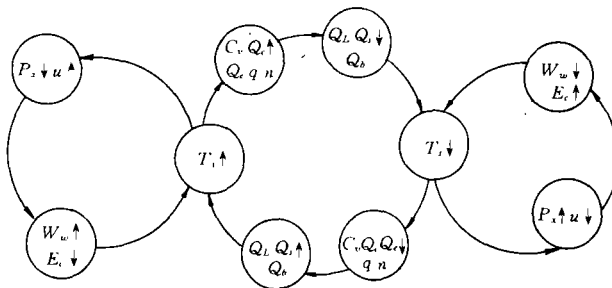


Fig. 7. Conceptual model of two feedback mechanisms in El Nino-La Nina cycle.  $P_z$ ,  $U$ ,  $C$ ,  $W_w$  and  $E_c$  denote zonal pressure gradient, zonal wind, tropical convergence, warm pool water and cold tongue water respectively.  $\uparrow$  denotes increasing, eastward expanding of warm pool water or strengthening of cold tongue water upwelling and  $\downarrow$  denotes decreasing.

and incident solar radiation reduced, and the net gain (loss) of heat decreased (increased) on the ocean surface from the central TPS to the western coast of Peru. During La Nina the circumstances were opposite.

(2) In the air-sea coupling process, both positive and negative feedback mechanisms involving the dynamic, thermal and hydrological processes interacted on and restrained each other to create favorable conditions for El Nino-La Nina cycle.

It should be pointed out that the two conclusions are based on the averaged situation of the concerned flow field and heat exchange anomalies in the El Nino and La Nina events. Because each El Nino (La Nina) has different beginning and ending time and its initial and ending states of the atmosphere and the ocean are also different, the SST, the flow fields and the heat exchange anomalies in each El Nino (La Nina) event under the action of the air-sea coupling are different. It is also true that their anomalies and variations are different in different developing stages of El Nino (La Nina) event .

#### REFERENCES

- Bjerknes, J. (1966). A possible response of the atmospheric Hadley circulation to equatorial anomalies of ocean temperature. *Tellus*, **18**: 820—829.
- Budyko, M.I. (1958). *The Heat Balance of the Earth's Surface*, English Translation by U.S. Weather Bureau, Washington, D.C., pp. 259
- Budyko, M.I. (1974). *Climate and Life*. Academic Press, pp. 508.
- Bunker, A. (1976). Computation of surface energy flux and annual air-sea interaction cycles of the North Atlantic Ocean. *Mon. Wea. Rev.*, **104**: 1121—1140.
- Ma Kaiyu et al. (1993). Study on air-sea heat exchange mechanism in El Nino and La Nina events. *Acta Meteor. Sinica*, **7**: 79—89.
- Monitoring Group of ENSO (1989). Classification and Index of El Nino Events. *Meteorological monthly*, **15**: 37—38 (in Chinese).
- Ramage, C.S. and Hori, A.M. (1981). Meteorological aspects of El Nino. *Mon. Wea. Rev.*, **109**: 1827—1835.
- Rowntree, P.R. (1972). The influence of tropical East Pacific Ocean temperature on the atmosphere. *Quart. J. Meteor. Soc.*, **98**: 290—321.
- Wang Shaowu et al. (1986). The western and central Pacific rainfall and the El Nino events. *Acta Meteor. Sinica*, **44**: 403—410 (in Chinese).
- Zhu Yafen and Yang Dasheng (1990). Analysis of air-sea heat exchange during 1983 El Nino. *Acta Oceanologica Sinica*, **12**: 167—178 (in Chinese).